

## Theory of the Wiedemann Effect

著者	YAMAMOTO Mikio
journal or publication title	Science reports of the Research Institutes, Tohoku University. Ser. A, Physics, chemistry and metallurgy
volume	10
page range	219-239
year	1958
URL	<a href="http://hdl.handle.net/10097/26874">http://hdl.handle.net/10097/26874</a>

# Theory of the Wiedemann Effect\*

Mikio YAMAMOTO

*The Research Institute for Iron, Steel and Other Metals*

(Received March 14, 1958)

## Synopsis

As regards the classical problem of the Wiedemann effect in polycrystalline ferromagnetics, any satisfactory theory has not yet been proposed, except Fromy's theory for the case of thin-walled circular tube specimens. We derive, in a simple way, a general expression for the Wiedemann effect or the torsion angle per unit length,  $\theta_r$ , of a cylindrical layer of the radius  $r$  in cylindrical rod of ferromagnetic substance, fixed at its one end and magnetized by a longitudinal magnetic field,  $H_l$ , parallel to, and by circular field,  $H_{cr}$ , around, its rod axis, and show that, when the elastic energy is negligible as compared with the magnetic field energy as in normal ferromagnetics, the general expression is reduced to

$$\theta_r = (2/r) \{ \lambda_l(H_r) - \lambda_t(H_r) \} (H_l H_{cr} / H_r^2) ,$$

where  $H_r = (H_l^2 + H_{cr}^2)^{1/2}$  and  $\lambda_l(H_r)$  and  $\lambda_t(H_r)$  are the longitudinal and transverse magnetostrictions accompanied with  $H_r$ . This expression may be written, for the surface of the rod of the radius  $a$ , as

$$\theta_a = (2/a) \{ \lambda_l(H_a) - \lambda_t(H_a) \} (H_l H_{ca} / H_a^2) ,$$

which holds also for a thin-walled tube and is the expression derived already by Fromy. This expression is further reduced to

$$\theta_a = (3/a) \cdot \lambda_l(H_a) \cdot (H_l H_{ca} / H_a^2)$$

when the volume magnetostriction may be negligible as in normal ferromagnetics. It is shown that the above expressions can explain, qualitatively completely and also to a considerable extent quantitatively, all of the available experimental facts concerning the Wiedemann effect.

## I. Introduction

The Wiedemann effect is a phenomenon that a ferromagnetic cylindrical rod or tube specimen fixed at its one end, twists around the rod or tube axis, when it is magnetized under the simultaneous action of longitudinal magnetic field,  $H_l$ , parallel to, and circular field,  $H_c$ , around the rod or tube axis, (Fig. 1). Since the circular magnetic field,  $H_c$ , is usually produced by the current,  $I$ , passing through the rod specimen itself or along the axis of the tube specimen, the relation  $H_c = 2I/a$  holds for the surface of the rod specimen or of the thin-walled tube specimen, where  $a$  is the radius of the rod or the outer radius of the thin-walled tube. Since this effect was found at first by Wiedemann<sup>(1)</sup> before the discovery of the

\* The 909 th report of the Research Institute for Iron, Steel and Other Metals. The original of this report written in Japanese language was published previously in *Ôyô-Butsuri* (J. Appl. Phys., Japan), **27** (1958), 88.

(1) G. Wiedemann; *Electrizität*, **3** (1881), 519 ("iron"; circular rods).

magnetostriction effect by Joule in 1842,<sup>(6)</sup> it has been the subject of numerous investigations.<sup>(2~11)</sup> In early days, it was recognized that this effect was associated with the magnetostriction effect,<sup>(3)</sup> and it was expected prematurely that there

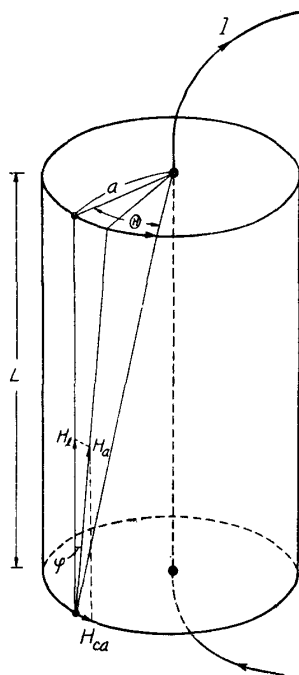


Fig. 1. To illustrate the Wiedemann effect in a cylindrical rod or tube specimen fixed at its lower end.

existed a relatively simple relation between the Wiedemann and longitudinal magnetostriction effects, but afterwards it was found that the state of affairs was not so simple.<sup>(4~6)</sup>

Theoretically the Wiedemann effect is simpler in thin-walled circular tube specimens than in circular rod ones, as will be shown later, but experimentally rod specimens are more favorite than tube specimens, as the former specimens are easily prepared. Consequently, experimental investigations have so far been made almost exclusively with rod specimens, except for a few ones (for example, by Williams<sup>(4)</sup>). General aspects of the effect are, however, common to both of the rod and tube specimens. Although materials with which the Wiedemann effect was measured are relatively scanty—iron, carbon steels, iron-aluminium alloys, nickel, and cobalt,<sup>(1,4,5,7,9~11)</sup> experimental facts obtained from the measurements

may be summarized as follows:—

I. If the longitudinal magnetic field,  $H_l$ , or the circular field,  $H_c$ , is zero, the Wiedemann effect does not occur, namely, the total torsion angle,  $\Theta$  (cf. Fig. 1) or the torsion angle per unit length of the specimen,  $\theta$  ( $= \Theta/L$ ;  $L$  = the length of the specimen), is zero.

II.  $\theta$  for iron, carbon steels, and alfer (13 %Al-Fe alloy) (for not so large  $H_l$  in all cases) and  $\theta$  for nickel and cobalt are different in sign (Figs. 2~4).

III.  $|\theta|$  are much larger for nickel and alfer than for iron and carbon steels (Figs. 2 and 3).

(2) Cf., for instance, S.R. Williams, *Magnetic Phenomena*, McGraw-Hill (1931).

(3) J.C. Maxwell, *Electricity and Magnetism*, 2 (1881), 87.

(4) S.R. Williams, *Phys. Rev.*, 32 (1911), 281 (low-carbon steel; circular tubes).

(5) S.R. Williams, *Phys. Rev.*, 10 (1917), 129 (theory).

(6) H.A. Pidgeon, *Phys. Rev.*, 13 (1919), 209 (Fe, Ni, Co; circular rods).

(7) P. McCorkle, *Phys. Rev.*, 22 (1923), 271 (Fe, Ni, Co; circular rods).

(8) E. Fromy, *J. de phys.*, [6] 7 (1926), 13 (theory).

(9) Y. Shirakawa, T. Ohara and T. Abe, *J. Japan Inst. Metals*, 16 (1952), 239; *Sci. Rep. RITU*, A9 (1957), 176 (13 %Al-Fe, Fe, Ni; circular rods).

(10) Y. Shirakawa, T. Ohara and T. Abe, *J. Japan Inst. Metals*, 16 (1952), 473; *Sci. Rep. RITU*, A9 (1957), 184 (13 %Al-Fe; circular rods; high temperatures).

(11) Y. Shirakawa, T. Ohara and T. Abe, *J. Japan Inst. Metals*, 20 (1956), 81 (Fe-Al; circular rods; high temperatures); *Sci. Rep. RITU*, in the present number.

IV. With increasing  $H_i$ ,  $|\theta(H_i)|$  rises at first quickly from zero and, after attaining the maximum value,  $|\theta(H_i)|_{max}$ , it falls slowly. The rate of its initial rapid rise increases with increasing  $H_e$ , though, in iron, it subsequently decreases (Figs. 2(a), 3(a) and 4(a)).

V.  $|\theta(H_i)|_{max}$  increases at first and then slowly with increasing  $H_e$  (Figs. 2(b) and 3(b)).

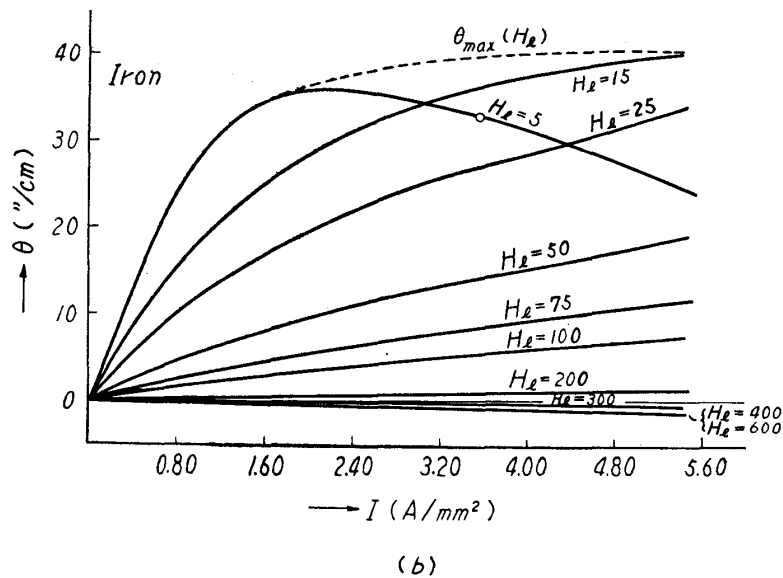
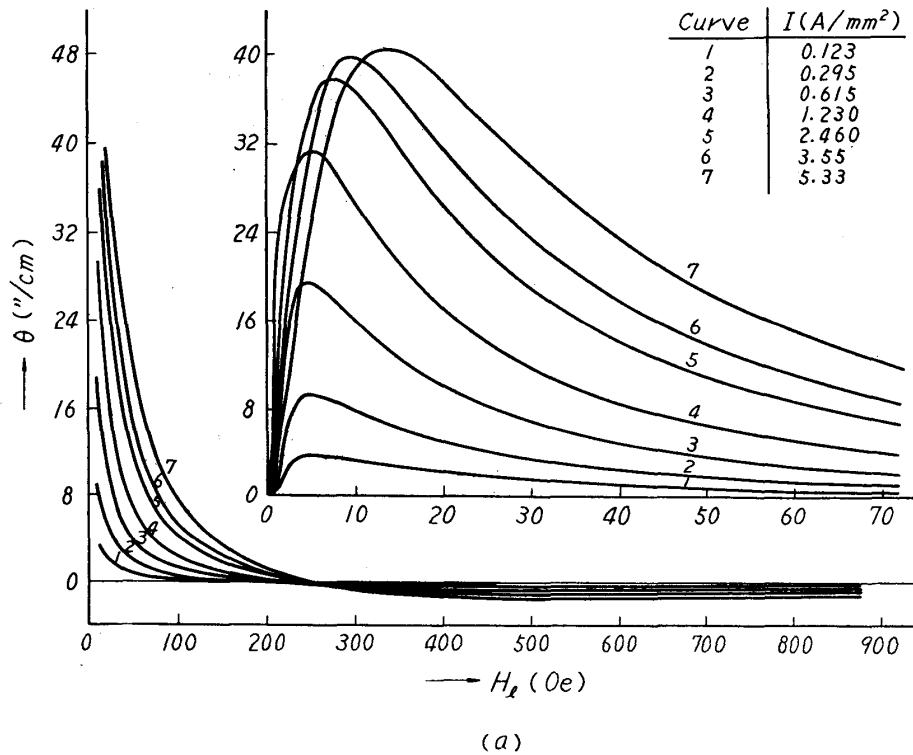


Fig. 2. Wiedemann effect in a cylindrical rod specimen of "iron" (possibly low carbon steel;  $a = 0.0512$  cm,  $L = 25.00$  cm; annealed at  $800^\circ C$  for 3 hours in a hydrogen stream)(Pidgeon(6)).  
 (a)  $\theta(H_i)$  curves and (b)  $\theta(I)$  curves.

VI. The value of  $H_i$  corresponding to  $|\theta(H_i)|_{max}$ , which is denoted as  $(H_i)_m^0$  hereafter, increases with increasing  $H_e$  (Figs. 2(a), 3(a), and 4).

VII. As  $H_i$  becomes larger,  $\theta(H_i)$  curves for alfer, nickel and cobalt tends monotonously to zero (Figs. 3(a) and 4), but the curves for iron and carbon steels

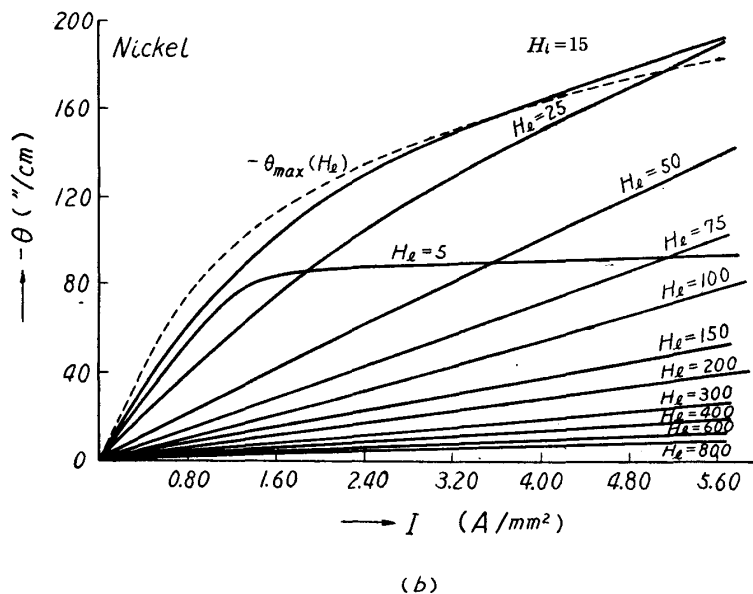
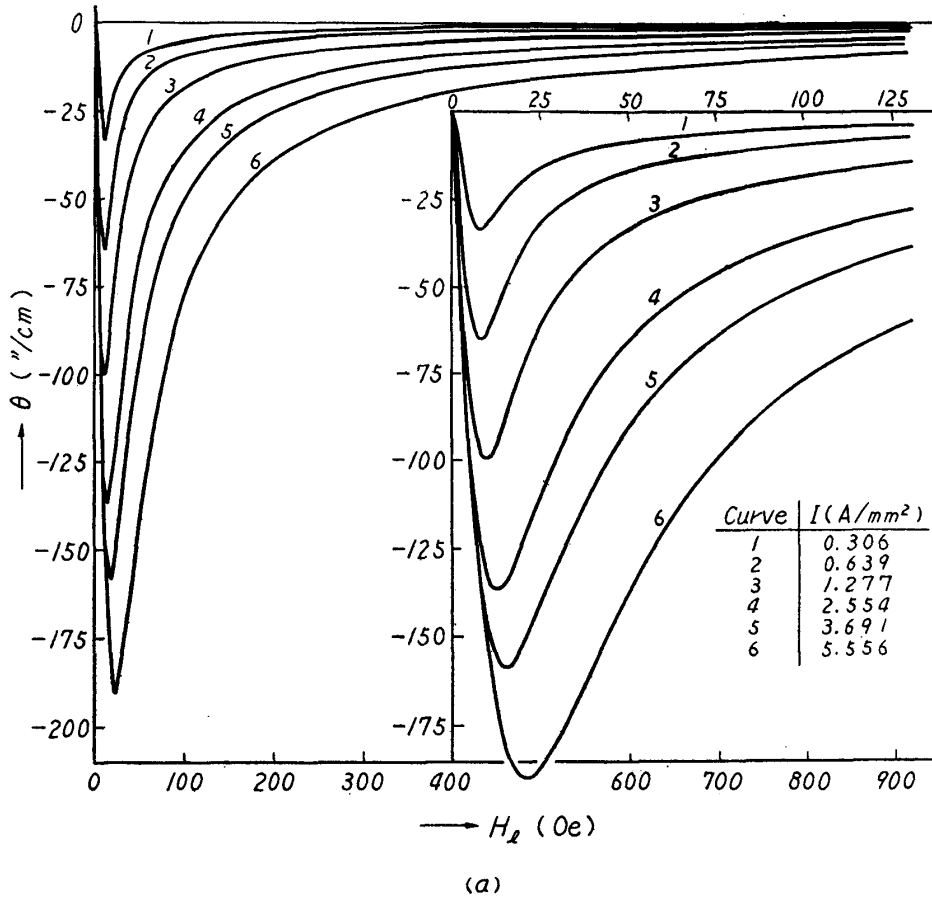


Fig. 3. Wiedemann effect in a cylindrical rod specimen of nickel ( $a = 0.0502$  cm,  $L = 25.01$  cm; annealed at  $800^\circ\text{C}$  for 3 hours in a hydrogen stream)(Pidgeon<sup>(6)</sup>). (a)  $\theta(H_i)$  curves and (b)  $\theta(I)$  curves.

pass through zero, changing from positive to negative, and tends to zero after making a flat minimum,  $\theta_{min}(H_i)$ ,  $|\theta_{min}(H_i)|$  increasing with increasing  $H_c$  (Fig. 2(a)).

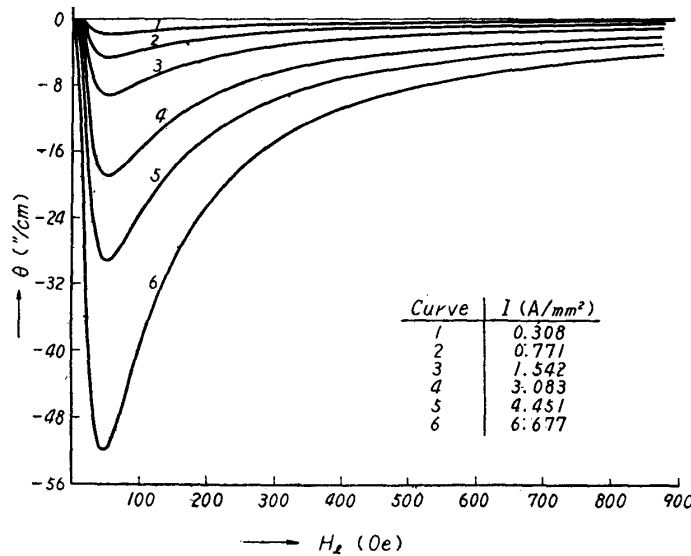


Fig. 4. Wiedemann effect in a cylindrical rod specimen of cobalt (98.71 % pure;  $a = 0.0456$  cm,  $L = 25.06$  cm; annealed at  $800^\circ\text{C}$  for 3 hours in a hydrogen stream)(Pidgeon<sup>(6)</sup>).

VIII. For iron and carbon steels,  $(H_i)_m^0$  is lower than the value of  $H_i$  where the longitudinal magnetostriction,  $\lambda_i$ , attains the maximum,  $H_m^\lambda$ , and the value of  $H_i$  where  $\theta(H_i)$  changes its sign,  $(H_i)_0^0$ , is lower than the value of  $H_i$  where  $\lambda_i$  changes its sign,  $H_0^\lambda$  (Fig. 5).

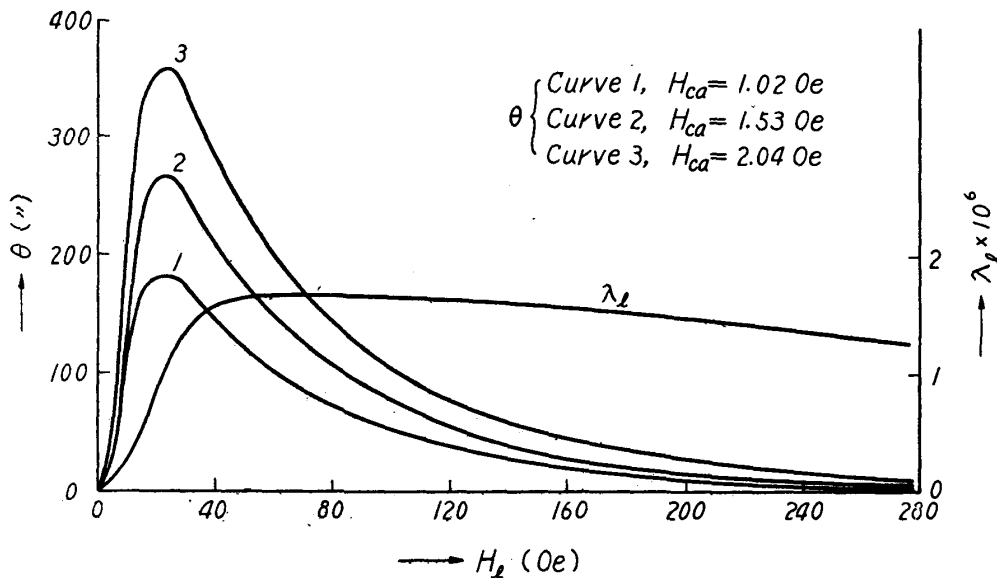


Fig. 5. Wiedemann effect and the longitudinal magnetostriction in a cylindrical tube specimen of low carbon steel (outer radius 0.2386 cm, inner radius 0.1538 cm,  $L = 80.2$  cm; heat-treatment unknown) (Williams<sup>(4)</sup>).

IX. The  $\theta(H_c)$  or  $\theta(I)$  curves takes roughly a linear course, of which the tangent increases at first and then decreases with increasing  $H_i$  (Figs. 2 (b) and

3(b)). Particularly in iron, the tangent of the curve for high  $H_l$  becomes negative (Fig. 2(b)). But, generally the  $\theta(H_l)$  or  $\theta(I)$  curve for low  $H_l$  deviates gradually from the linearity and approaches to the abscissa as  $H_l$  or  $I$  becomes larger.

X. The Wiedemann effect in the rod specimen varies appreciably with its diameter.<sup>(6)</sup>

XI. The Wiedemann effect shows hysteresis.<sup>(6)</sup>

Now, theories of the Wiedemann effect have so far been proposed by Williams,<sup>(5)</sup> Pidgeon,<sup>(6)</sup> and Fromy.<sup>(8)</sup> Williams'<sup>(5)</sup> theory is as follows:— When longitudinal magnetic field,  $H_l$ , and circular field,  $H_c$ , act simultaneously on a ferromagnetic circular thin-walled tube of the radius  $a$  and the length  $L$ , both fields combine to produce the resultant field,  $H$ , making an angle  $\varphi$  against  $H_l$  (cf. Fig. 1), which is given by

$$H = (H_l^2 + H_c^2)^{1/2} \quad \text{and} \quad \tan \varphi = H_c/H_l. \quad (1)$$

The longitudinal magnetostriction,  $\lambda_l(H)$ , corresponding to this resultant field produces a change in length along a spiral inclined by the angle  $\varphi$  to the generating line of the tube and hence the displacement by  $(L/\cos \varphi)\lambda_l(H)$  of the free end of the spiral, the component perpendicular to the tube axis or  $H_l$  of this displacement resulting the torsion,  $\theta$ , per unit length of the tube, which is given by

$$\theta = \{\lambda_l(H)/a\} \tan \varphi = \{\lambda_l(H)/a\} (H_c/H_l). \quad (2)$$

As pointed out already by Fromy,<sup>(8)</sup> this expression (2) can describe "qualitatively"<sup>(12)</sup> the general aspects for large  $H_l$  of the Wiedemann effect, but, for small  $H_l$ , it disagrees with the experimental facts, and, in particular for  $H_l = 0$ , it yields  $\theta = \infty$ , which contradicts to the fundamental experimental fact I mentioned above.

Next, Pidgeon<sup>(6)</sup> considered that a point in a circular rod distant by  $r$  from the rod axis, displaces by  $L\lambda_l(H_r)$  owing to  $\lambda_l(H_r)$  corresponding to the resultant field  $H_r$  along the direction making an angle  $\varphi$  with  $H_l$ , and thus he derived the expression

$$\theta = \{\lambda_l(H)/r\} (H_c/H) = \{\lambda_l(H)/r\} \{H_c/(H_l^2 + H_c^2)^{1/2}\}, \quad (3)$$

which also contradicts to the fundamental experimental fact I, since it yields  $\theta = \lambda_l(H_{ca})/r \neq 0$  for  $H_l = 0$ . Williams<sup>(5)</sup> and Pidgeon<sup>(6)</sup> as well regarded the magnetostriction as a vector quantity, which is the fatal defect.

On the contrary, taking into consideration of the transverse magnetostriction,  $\lambda_t$ , in addition to the longitudinal magnetostriction,  $\lambda_l$ , and based on the fact that, when a tube is twisted, a point on its circumference remains on the same circumference as when untwisted, Fromy<sup>(8)</sup> derived, through an elementary and hence lengthy consideration, the following expression for the Wiedemann effect in the case of the thin-walled tube specimen:

(12) Although Fromy used the word "qualitatively", it may be replaced by the word "quantitatively", as seen from Section III.

$$\theta = (2/a) \{ \lambda_l(H) - \lambda_t(H) \} \cdot H_l H_c / H^2, \quad (4)$$

which is valid for sufficiently small  $\theta$ .<sup>(13)</sup> This expression not only yields  $\theta = 0$  for  $H_l = 0$  or  $H_c = 0$ , but also describes "qualitatively"<sup>(12)</sup> well other experimental facts. Although Fromy's theory has been almost entirely neglected in the literature possibly because of the lack of quantitatively perfect agreement with the experimental data,<sup>(14)</sup> it essentially treats the magnetostriction as a tensor quantity and thus it may be correct, as shown later (Section II).

In the following, we derive the expression for the Wiedemann effect in the circular rod specimen, simply by regarding the magnetostriction as the tensor, and shows that the expression thus derived may be reduced to Fromy's expression (4) for the thin-walled tube specimen as a limiting case, that the Wiedemann effect in the rod specimen can also be expressed practically by the expression (4), and that the expression

$$\theta = (3/a) \cdot \lambda_l(H) \cdot H_l H_c / H^2 \quad (4a)$$

as simplified from the expression (4) under the condition

$$\lambda_t = -\lambda_l/2 \quad (5)$$

which means that the volume magnetostriction is negligible, can describe qualitatively and also quantitatively well all of the available experimental facts.

## II. Derivation of the theoretical formulae

At a point P distant by  $r$  from the rod axis in a circular rod of the radius  $a$ , fixed at its lower end, the longitudinal magnetic field,  $H_l$ , acts in the direction of the rod axis and the circular field,  $H_{cr}$ , acts in the direction of the tangent to the circle of the radius  $r$  passing through P (Fig. 6(a)), the resultant field,  $H_r = (H_l^2 + H_{cr}^2)^{1/2}$ , being in the direction making an angle  $\varphi_r = \tan^{-1}(H_{cr}/H_l)$  with the direction of  $H_l$ . The direction of the magnetization,  $I$ , at this point does not coincide with that of the resultant field,  $H_r$ , because of the elastic constraint of material outside and inside the cylinder passing through, P, but, by the reason of symmetry, it is in the plane  $(H_l, H_{cr})$ , making a small angle,  $\varepsilon_r$ , with the direction of  $H_r$ .

The components along the direction of  $I_r$  and along a direction perpendicular to the direction of  $I_r$  of the magnetostriction associated with the magnetization,  $I_r$ , are  $\lambda_l(I_r)$  and  $\lambda_t(I_r)$ . In other words, the components of the magnetostriction tensor at P, referred to the rectangular coordinate system  $(\xi, \eta, \zeta)$  which is obtained by rotating by an angle  $-(\varphi_r + \varepsilon_r)$  about the  $z$  axis the rectangular coordinate system  $(x, y, z)$ , of which the  $z$  axis is the rod axis of the cylinder and the  $x$  axis is the radius of the cylinder passing through P, are as follows:

(13) All of the Wiedemann effects so far observed satisfy this condition.

(14) It is shown later (Section IV) that the quantitatively perfect comparison of theory and experiment regarding the Wiedemann effect is impossible at present.



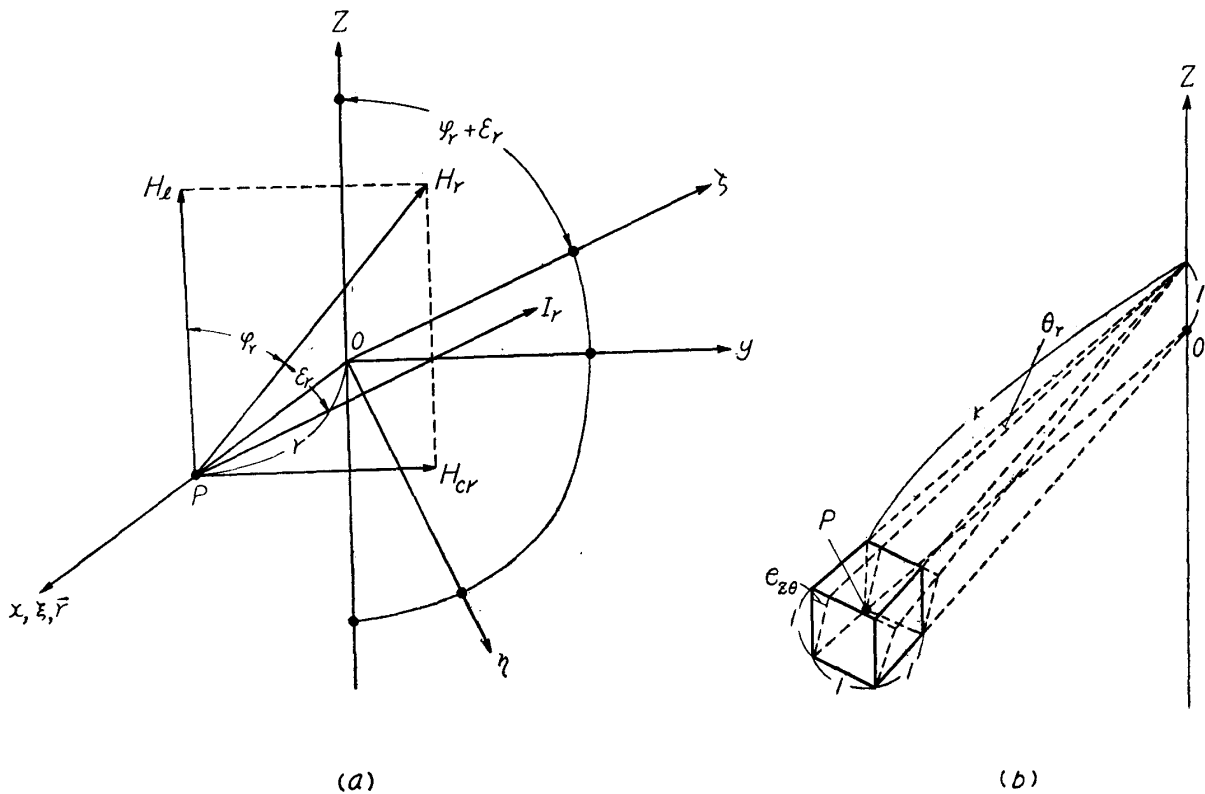


Fig. 6. To illustrate the theory of the Wiedemann effect.

$$e_{\xi\xi} = e_{\eta\eta} = \lambda_t(I_r), \quad e_{\zeta\zeta} = \lambda_l(I_r), \quad \text{and} \quad e_{\xi\eta} = e_{\xi\zeta} = e_{\eta\zeta} = 0. \quad (6)$$

Then, the components of the magnetostriction tensor referred to the cylindrical coordinate system  $(r, \theta, z)$  of which the  $r$  axis is the  $\xi$  axis are as follows:

$$\left. \begin{aligned} e_{rr} &= \lambda_t(I_r), \\ e_{\theta\theta} &= \{\lambda_l(I_r) \cdot I_{rc}^2 + \lambda_t(I_r) \cdot I_{rl}^2\} / I_r^2, \\ e_{zz} &= \{\lambda_l(I_r) \cdot I_{rl}^2 + \lambda_t(I_r) \cdot I_{rc}^2\} / I_r^2, \\ e_{\theta z} &= 2\{\lambda_l(I_r) - \lambda_t(I_r)\} \cdot I_{rl} I_{rc} / I_r^2, \end{aligned} \right\} \quad (7)$$

and

$$e_{r\theta} = e_{rz} = 0,$$

where

$$I_{rl} = I_r \cos(\varphi_r + \varepsilon_r) \quad \text{and} \quad I_{rc} = I_r \sin(\varphi_r + \varepsilon_r).$$

Of these components,  $e_{rr}$ ,  $e_{\theta\theta}$ , and  $e_{zz}$  are simple strains along the directions of the radius, perpendicular to the rod axis, and of the rod axis, respectively, and  $e_{\theta z} = e_{z\theta}$  is the shear along the directions of the rod axis or perpendicular to it, of the unit volume at P. Since this unit volume may be regarded as fixed at its lower face (Fig. 6(b)), the following torsion occurs corresponding to  $e_{z\theta}$ :

$$\theta_r = e_{z\theta} / r = (2/r) \{\lambda_l(I_r) - \lambda_t(I_r)\} \cdot (I_{rl} I_{rc} / I_r^2). \quad (8)$$

This torsion is the Wiedemann effect.

Now, the magnetization  $I_r$  takes a direction in which the sum of the magnetic field energy,  $E_m$ , and of the elastic energy,  $E_e$ , is minimum. Accordingly, in the case where  $E_e$  need not be considered as in a thin-walled tube,  $\epsilon_r = 0$ , which reduces Eq. (8) to Fromy's expression (4).

$E_m$  and  $E_e$  are given, respectively, by

$$E_m = -I_r H_r \cos \epsilon_r \quad (9)$$

and

$$E_e = (C_1/2)(e_{rr} + e_{\theta\theta} + e_{zz})^2 + G(e_{rr}^2 + e_{\theta\theta}^2 + e_{zz}^2 + 2e_{r\theta}^2 + 2e_{\theta z}^2 + 2e_{rz}^2), \quad (10)$$

where  $C_1 = G(E - 2G)/(3G - E)$ , and  $E$  and  $G$  are Young's modulus and the rigidity modulus, respectively. Substituting Eq. (7) into Eqs. (10), we get

$$E_e = (C_1/2)\{\lambda_l(I_r) + 2\lambda_t(I_r)\}^2 + G[\lambda_l^2(I_r) + 2\lambda_t^2(I_r) + 6\{\lambda_l(I_r) - \lambda_t(I_r)\}^2]\sin^2(\varphi_r + \epsilon_r)\cos^2(\varphi_r + \epsilon_r). \quad (10a)$$

For normal ferromagnetic substances, since  $I_r \cong 10^2 \sim 10^3$  gauss for  $H_r \cong 1$  Oe,  $E_m \cong 10^2 \sim 10^3$  ergs/cm<sup>3</sup>, and, since  $C_1 \cong G \cong 10^{12}$  dynes/cm<sup>2</sup> and  $\lambda_l \cong -2\lambda_t \cong 10^{-6}$ ,  $E_e \cong 1$  erg/cm<sup>3</sup>,  $E_e$  being much smaller than  $E_m$ . Then, practically  $\epsilon_r = 0$ , and thus Eq. (8) may be reduced to

$$\theta_r = (2/r)\{\lambda_l(H_r) - \lambda_t(H_r)\} \cdot (H_l H_{cr}/H_r^2), \quad (11)$$

which becomes, for the surface of the rod ( $r = a$ ),

$$\theta_a = (2/a)\{\lambda_l(H_a) - \lambda_t(H_a)\} \cdot (H_l H_{ca}/H_a^2). \quad (12)$$

Eq. (12), which holds also for a thin-walled tube of the radius  $a$ , is the expression derived already by Fromy,<sup>(8)</sup> as mentioned before. Further, if the volume magnetostriction may be neglected or  $\lambda_t = -\lambda_l/2$  as in normal ferromagnetics, Eq. (12) is reduced simply to

$$\theta_a = (3/a) \cdot \lambda_l(H_a) \cdot (H_l H_{ca}/H_a^2). \quad (13)$$

### III. Analysis of the theoretical formulae and the qualitative comparison with the experimental facts

Eq. (12) or (13) indicates that the Wiedemann effect in the circular rod or tube specimen is determined uniquely by the radius of the specimen and its magnetostriction characteristics. Accordingly, the hysteresis of the magnetostriction manifests itself as that of the Wiedemann effect, which is the experimental fact XI mentioned in Section I. Also, the Wiedemann effect in the same substance varies with the diameter of the specimen, which is the experimental fact X.

Eq. (12) or (13) yield  $\theta_a = 0$  when  $H_c = \text{constant}$  and  $H_l = 0$  or  $\infty$  or when  $H_l = \text{constant}$  and  $H_c = 0$  or  $\infty$ .  $\theta_a = 0$  when  $H_c = \text{constant}$  and  $H_l = 0$  or when  $H_l = \text{constant}$  and  $H_c = 0$  is the fundamental experimental fact I, and  $\theta_a = 0$  when  $H_c = \text{constant}$  and  $H_l = \infty$  is a part of the experimental fact III, while  $\theta_a = 0$  when  $H_l = \text{constant}$  and  $H_c = \infty$  has not yet been evidenced experimentally since experimenting using sufficiently large  $H_c$  is very difficult.

$\lambda_l(H_a) - \lambda_t(H_a)$  for small  $H_a$  is positive in iron, while it is negative and its absolute value is large in nickel. Then, Eq. (12) or (13) indicates that, for the same configuration of  $H_l$  and  $H_{ca}$ , the Wiedemann effect of iron are different in sign from that of nickel and the latter is larger in absolute magnitude than the former, which are the experimental facts II and III cited in Section I.

For  $H_l \ll H_{ca}$ , Eq. (12) is reduced to

$$\theta_a = (2/a) \{ \lambda_l(H_{ca}) - \lambda_t(H_{ca}) \} \cdot (H_l/H_{ca}), \quad (12a)$$

which indicates that the Wiedemann effect is proportional to  $H_l$  for  $H_l \ll H_{ca}$ . But, this has not yet been recognized, since the value of  $H_{ca}$  taken in the experiments so far made is small, as stated above, so that the measured points for  $H_l$  are few. On the contrary, for  $H_{ca} \ll H_l$ , Eq. (12) is reduced to

$$\theta_a = (2/a) \{ \lambda_l(H_a) - \lambda_t(H_a) \} \cdot (H_{ca}/H_l), \quad (12b)$$

which shows that the Wiedemann effect is proportional to  $H_{ca}$  for  $H_{ca} \ll H_l$ , and this is a part of the experimental fact IX.

Hereafter we consider, for simplicity, only with Eq. (13). In order to analyse Eq. (13) in more detail, it is at first necessary to distinguish the types of the  $\lambda_l(H)$

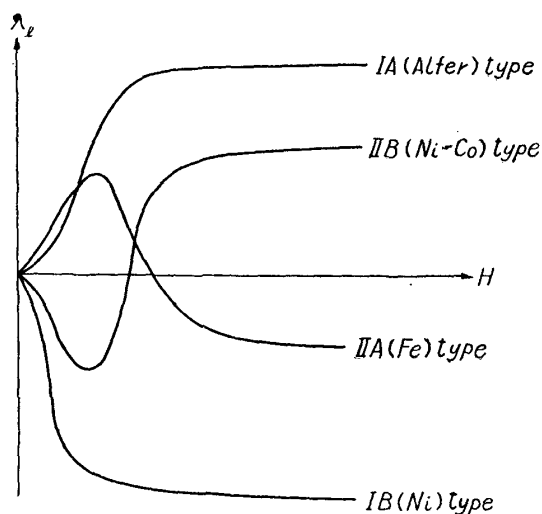


Fig. 7. Types of  $\lambda_l(H)$  curves.

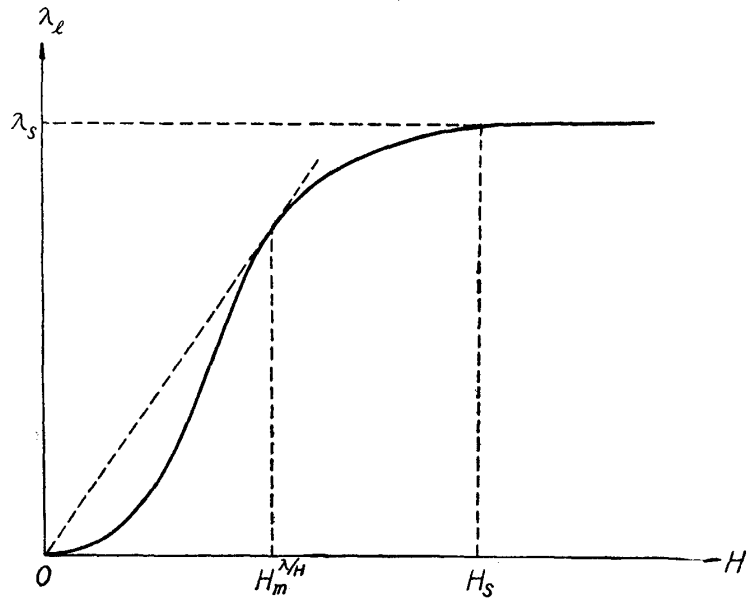
or longitudinal magnetostriction vs. magnetic field curves. There are two main types of the  $\lambda_l(H)$  curves, as shown in Fig. 7. The I type involves the  $\lambda_l(H)$  curves which are positive over the whole range of magnetic field and rise monotonously with increasing field, as in 13% Al-Fe alloy (alfer), and the curves which are negative over the whole range of field and whose  $|\lambda_l|$  increases monotonously with increasing field, as in nickel. We shall call the former case the IA type and the latter the IB type, respectively. The II type involves the curves which are positive in the weak field range but

fall after passing a maximum, becoming negative in the strong field range, as in iron, and the curves which are negative in the weak field range but rise after passing a minimum, becoming positive, as in 30% Co-Ni alloy. We shall call the former and latter types as the IIA and IIB types, respectively.

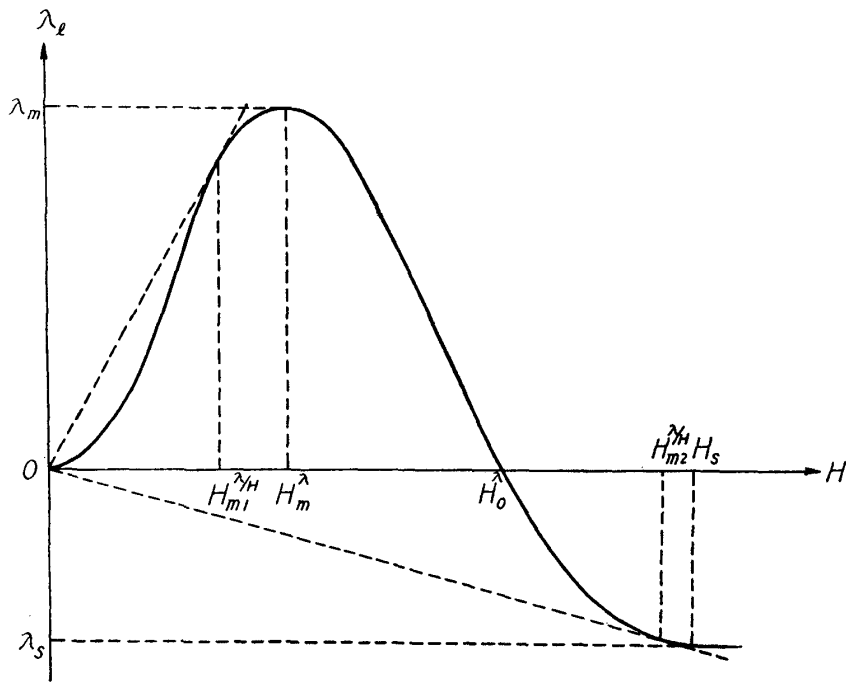
The IA (or IB)-type  $\lambda_l(H)$  curve starts horizontally from the origin, passes through an inflexion point, and finally attains a positive (or negative)<sup>(15)</sup> saturation value,  $\lambda_s$ , at  $H = H_s$ ,  $\lambda_l(H)/H$  showing a positive maximum (or negative minimum) at a certain value of  $H$ ,  $H_m^{\lambda/H}$  (Fig. 8(a)). Thus,

$$\lambda_l(H) \geq (\text{or } \leq) 0 \quad \text{and} \quad d\lambda_l(H)/dH \geq (\text{or } \leq) 0, \quad (14)$$

(15) Such a description as  $\text{---}$  (or  $\text{---}$ ) corresponds to IA (or IB) or IIA (or IIB).



(a)



(b)

Fig. 8. Characteristics of  $\lambda_i(H_i)$  curves of the IA and IIA types.  
 (a) IA type and (b) IIA type

in the whole range of  $H$ ,

$$\lambda_l(H)|_{H=0} = 0 \quad \text{and} \quad d\lambda_l(H)/dH|_{H=0} = 0, \quad (15)$$

$$\lambda_l(H)|_{H \geq H_s} = \lambda_s \quad \text{and} \quad d\lambda_l(H)/dH|_{H \geq H_s} = 0, \quad (16)$$

and

$$\lambda_l(H)/H|_{H=H_m^\lambda/H} = d\lambda_l(H)/dH|_{H=H_m^\lambda/H}. \quad (17)$$

The IIA (or IIB)-type  $\lambda_l(H)$  curve also starts horizontally from the origin, passes through an inflexion point, attains a positive maximum (or negative) minimum,  $\lambda_m$ , then falls (or rises), cuts the  $H$  axis at  $H = H_0$ , and finally attains a negative (or positive) saturation value,  $\lambda_l(H)/H$  showing first a positive maximum (or negative) minimum at  $H = H_{m1}^\lambda/H$ , and then a negative minimum (or positive) maximum at  $H = H_{m2}^\lambda/H$  (Fig. 8(b)). Thus, Eq. (14) holds for  $0 \leq H \leq H_m^\lambda$ , and

$$\lambda_l(H) \geq (\text{or} \leq) 0 \quad \text{and} \quad d\lambda_l(H)/dH \leq (\text{or} \geq) 0 \quad \text{for} \quad H_m^\lambda \leq H \leq H_0^\lambda, \quad (18a)$$

and

$$\lambda_l(H) \leq (\text{or} \geq) 0 \quad \text{and} \quad d\lambda_l(H)/dH \leq (\text{or} \geq) 0 \quad \text{for} \quad H \geq H_0^\lambda. \quad (18b)$$

Moreover, Eqs. (15) and (16) hold as well, and

$$\lambda_l(H)|_{H=H_m^\lambda} = \lambda_m \quad \text{and} \quad d\lambda_l(H)/dH|_{H=H_m^\lambda} = 0, \quad (19)$$

$$\lambda_l(H)|_{H=H_0^\lambda} = 0 \quad \text{and} \quad d\lambda_l(H)/dH|_{H=H_0^\lambda} < (\text{or} >) 0, \quad (20)$$

$$\lambda_l(H)/H|_{H=H_{m1}^\lambda/H} = d\lambda_l(H)/dH|_{H=H_{m1}^\lambda/H}, \quad (21a)$$

$$\lambda_l(H)/H|_{H=H_{m2}^\lambda/H} = d\lambda_l(H)/dH|_{H=H_{m2}^\lambda/H}, \quad (21b)$$

and

$$H_{m1}^\lambda/H < H_0^\lambda < H_{m2}^\lambda/H. \quad (22)$$

It is to be noted that, as may be seen from mentioned before, there are Wiedemann effects of the IA, IB, IIA, and IIB types corresponding to the types of the magnetostriction curves.

Further, we assume that, in Eq. (13),  $\theta_a \geq 0$  according to  $\lambda_l \geq 0$  when  $H_l$  and  $H_{ca}$  are taken as shown in Figs. 1 and 6. Then, in the following analysis, we may consider  $|\theta_a|$  and  $|\lambda_l|$  connected by the equation:

$$|\theta_a| = (3/a) \cdot |\lambda_l(H_a)| \cdot (H_l H_{ca} / H_a^2). \quad (13a)$$

#### A. Characteristics of the $\theta_a(H_l)$ curve.

In the first place, we get, from Eq. (13a),

$$d|\theta_a(H_l)|dH_l = (3/a) (H_{ca}/H_a^3) [\{d|\lambda_l(H_a)|/dH_a\} H_l^2 + \{|\lambda_l(H_a)|/H_a\} (H_{ca}^2 - H_l^2)]. \quad (23a)$$

(1) Slope at the origin,  $d|\theta_a(H_l)|/dH_l|_{H_l=0}$ .

We obtain, from Eq. (23a),

$$d|\theta_a(H_l)|/dH_l|_{H_l=0} = (3/a) \cdot \{|\lambda_l(H_{ca})|/H_{ca}\}, \quad (24a)$$

which indicates that, as  $H_{ca}$  increases from zero, the slope at the origin of the  $\theta_a(H_l)$  curve increases (or decreases) from zero, attains a positive maximum (or

negative minimum) at  $H_{ca} = H_m^{\lambda/H}$  or  $H_{m1}^{\lambda/H}$  and then decreases (or increases), and, in the IIA (or IIB)-type Wiedemann effect, it afterwards passes through zero at  $H_{ca} = H_0^\lambda$ , attains a negative minimum (or positive maximum) at  $H_{ca} = H_{m2}^{\lambda/H}$ , and finally approaches to zero as  $H_{ca} \rightarrow \infty$ . Experimentally, because of the before-mentioned smallness of the experimental range of  $H_{ca}$ , only it has been known that  $d|\theta_a(H_i)|/dH_i|_{H_i=0}$  increases with increasing  $H_{ca}$  and, in iron, it then decreases, which is a part of the above-mentioned experimental fact IV.

(2) Extreme values,  $\theta_m(H_i)$ , and the corresponding  $H_i$  value,  $(H_i)_m^0$  in the Wiedemann effects of the I and II types in the field range  $H_a < H_m^\lambda$ .

It also follows from Eq. (23a) that the  $\theta_a(H_i)$  curve reaches an extreme value  $\theta_m(H_i)$  at the value of  $H_i$ ,  $(H_i)_m^0$ , which satisfies the following relation:

$$d|\lambda_i(H_a)|/dH_a|_{H_i=(H_i)_m^0} = |\lambda_i(H_a)|/H_a|_{H_i=(H_i)_m^0} \cdot [\{(H_i)_m^0\}^2 - H_{ca}^2]/\{(H_i)_m^0\}^2. \quad (25a)$$

The IA (or IB)-type Wiedemann effect has only one value of  $(H_i)_m^0$ ,  $\theta_m(H_i)$  being a positive maximum (or negative minimum), while the IIA (or IIB)-type effect has two values of  $(H_i)_m^0$ ,  $\theta_{m1}(H_i)$  at  $H_i = (H_i)_{m1}^0$  and  $\theta_{m2}(H_i)$  at  $H_i = (H_i)_{m2}^0$  being, respectively, a positive maximum (or negative minimum) and a negative minimum (or positive maximum). These are parts of the above-cited experimental facts IV and VII.

As mentioned before, in the whole field range of the IA (or IB)-type Wiedemann effect and in the field range  $0 \leq H_a \leq H_m^\lambda$  of the IIA (or IIB)-type effect, Eq. (14) holds, so that we get, from Eq. (25a),

$$(H_i)_m^0 \text{ or } (H_i)_{m1}^0 \geq H_{ca} \quad \text{for} \quad 0 \leq H_a \leq H_s \text{ or } H_m^\lambda. \quad (26a)$$

$(H_i)_m^0$  or  $(H_i)_{m1}^0 = H_{ca}$  realizes in the case where  $d|\lambda_i(H_a)|/dH_a = 0$ , namely, the value of  $H_a$  corresponding to  $(H_i)_m^0$ ,  $(H_a)_m^0$ , is equal to or greater than  $H_s$  or equal to  $H_m^\lambda$ . Thus, as  $H_{ca}$  increases from zero,  $(H_i)_m^0$  and  $(H_i)_{m1}^0$  increases, respectively, from  $H_m^{\lambda/H}$  and  $H_{m1}^{\lambda/H}$ , as may be seen from Eq. (25a), which, experimentally, has been known qualitatively (the experimental fact VI). And,  $(H_i)_m^0$  reaches to  $H_s/\sqrt{2}$ , after which it increases proportionally to  $H_{ca}$ , while  $(H_i)_{m1}^0$  reaches to  $H_m^\lambda/\sqrt{2}$ . Or,

$$H_m^{\lambda/H} < (H_i)_m^0 \leq H_s/\sqrt{2} < H_s \quad \text{and} \quad H_{m1}^{\lambda/H} < (H_i)_{m1}^0 \leq H_m^\lambda/\sqrt{2} < H_m^\lambda. \quad (27a)$$

The latter expression in Eq. (27a) indicates that, in iron,  $(H_i)_{max}^0 < H_m^\lambda$ , which is a part of the before-cited experimental fact VIII.

In the case where  $H_{ca} \ll (H_i)_m^0$  or  $(H_i)_{m1}^0$ , namely  $(H_a)_m^0 \cong (H_i)_m^0$ , it follows from Eq. (25a) that  $d|\lambda_i(H_a)|/dH_a|_{H_i=(H_i)_m^0} = |\lambda_i\{(H_i)_m^0\}|/(H_i)_m^0 = \{|\lambda_i(H_a)|/H_a\}_m$ , ( $\{|\lambda_i(H_a)|/H_a\}_m$  expresses an extreme value of  $|\lambda_i(H_a)|/H_a$ ), so that we get, from Eq. (13a),

$$\left. \begin{aligned} |\theta_m(H_i)| &= (3/a) \{|\lambda_i(H_a)|/H_a\}_m \cdot H_{ca} \quad \text{for} \quad H_{ca} \ll (H_i)_m^0 \\ \text{and} \quad |\theta_{m1}(H_i)| &= (3/a) \{|\lambda_i(H_a)|/H_a\}_{m1} \cdot H_{ca} \quad \text{for} \quad H_{ca} \ll (H_i)_{m1}^0. \end{aligned} \right\} \quad (28a)$$

On the contrary, in the case where  $H_{ca} = (H_i)_m^0 = [\{(H_a)_m^0\}^2 - H_{ca}^2]^{1/2} \geq H_s/\sqrt{2}$ ,  $(H_a)_m^0 \geq H_s$ , and in the case where  $H_{ca} = (H_i)_{m1}^0 = \{[(H)_{m1}^0]^2 - H_{ca}^2\}^{1/2} = H_m^\lambda/\sqrt{2}$ ,  $(H_a)_{m1}^0 = H_m^\lambda$ , so that we get, from Eq. (13a)

$$\left. \begin{aligned} |\theta_m(H_i)| &= (3/2a) \cdot |\lambda_s| & \text{for } H_{ca} = (H_i)_m^0 \geq H_s/\sqrt{2} \\ \text{and } |\theta_m(H_i)| &= (3/2a) \cdot |\lambda_m| & \text{for } H_{ca} = (H_i)_{m1}^0 = H_m^\lambda/\sqrt{2} \end{aligned} \right\} \quad (29a)$$

Thus, as  $H_{ca}$  increases from zero,  $\theta_m(H_i)$  or  $\theta_{m1}(H_i)$  starts from zero and increases (or decreases) at first in proportion to  $H_{ca}$ , but afterwards the rate of increase (or decrease) decreases gradually,  $\theta_m(H_i)$  or  $\theta_{m1}(H_i)$  finally attaining saturation. This is the experimental fact V mentioned in Section I.

(3)  $\theta_m(H_i)$  and  $(H_i)_m^0$  of the II-type Wiedemann effect in the field range  $H_a \geq H_m^\lambda$ .

For the IIA (or IIB)-type Wiedemann effect in the field range  $H_m^\lambda \leq H_a \leq H_0^\lambda$ , Eq. (18a) holds, as mentioned before, so that we get, from Eq. (25a),

$$(H_i)_{m1}^0 \leq H_{ca} \quad \text{for } H_m^\lambda \leq H_a \leq H_0^\lambda. \quad (30a)$$

Consequently, for  $H_{ca} > (H_i)_{m1}^0$ ,  $\lambda_l(H_i)|_{H_i=(H)_{m1}^0} \geq$  (or  $\leq$ ) 0, and hence  $(H_a)_{m1}^0 \leq (H_a)_0^\lambda$ . Thus, as  $H_{ca}$  increases from  $H_m^\lambda/\sqrt{2}$ ,  $(H_i)_{m1}^0$  decreases from  $H_m^\lambda/\sqrt{2}$  and vanishes when  $H_{ca}$  attains to  $H_0^\lambda$ . Also, for  $H_{ca} \gg (H_i)_{m1}^0$ , we have, from Eq. (13a),

$$|\theta_{m1}(H_i)| = (3/a) \cdot |\lambda_l(H_{ca})| \cdot (H_i)_{m1}^0/H_{ca} \quad \text{for } H_{ca} \gg (H_i)_{m1}^0, \quad (31a)$$

which indicates that, as  $H_{ca}$  increases from  $H_m^\lambda/\sqrt{2}$ ,  $\theta_{m1}(H_i)$  decreases (or increases) from  $(3/2a)\lambda_m$  and vanishes at  $H_{ca} = H_0^\lambda$ . Such changes of  $(H_i)_{m1}^0$  and  $\theta_{m1}(H_i)$  when  $H_{ca} > (H_i)_{m1}^0$ , however, have not yet been observed experimentally because of the above-mentioned lack of the measured range of  $H_{ca}$ .

Further, in the IIA (or IIB)-type Wiedemann effect,  $\theta_a(H_i)$  becomes zero once at  $H_a = H_0^\lambda$ , as seen from Eq. (13), and, since  $H_0^\lambda = [\{(H_i)_0^0\}^2 + H_{ca}^2]^{1/2}$ , we get

$$(H_i)_0^0 < H_0^\lambda = (H_a)_0^\lambda|_{H_{ca}=0} = (H_i)_0^\lambda. \quad (32a)$$

Thus, as  $H_{ca}$  increases, the value of  $H_i$  where  $\theta_a(H_i)$  once becomes zero,  $(H_i)_0^0$ , decreases from  $H_0^\lambda$ , and vanishes at  $H_{ca} = H_0^\lambda$ , namely,  $(H_i)_0^0$  is always lower than  $(H_i)_0^\lambda$ , which is a remaining part of the experimental fact VIII cited before.

Finally, in the field range  $H_a \geq H_0^\lambda$ , Eq. (18b) holds, so that we have, from Eq. (25a),

$$(H_i)_{m2}^0 \geq H_{ca} \quad \text{for } H_a \geq H_0^\lambda. \quad (33a)$$

Thus, similarly to the cases of  $(H_i)_m^0$  and  $(H_i)_{m1}^0$  mentioned in (2), as  $H_{ca}$  increases from zero,  $(H_i)_{m2}^0$  increases from  $H_m^{N/H}$  to  $H_s/\sqrt{2}$  and then increases in proportion to  $H_{ca}$ , but this has not yet been confirmed experimentally because of the extreme flatness of the negative minimum (or positive maximum). Further, we have, similarly to the cases of  $\theta_m(H_i)$  and  $\theta_{m1}(H_i)$ ,

$$|\theta_{m2}(H_i)| = (3/a) \{ |\lambda_i(H_a)|/H_a \}_{m2} \cdot H_{ca} \quad \text{for } H_{ca} \ll (H_i)_{m2}^0 \quad (34a)$$

and

$$|\theta_{m2}(H_i)| = (3/2a) \cdot |\lambda_s| \quad \text{for } H_{ca} = (H_i)_{m2}^0 \geq H_s/\sqrt{2} . \quad (35a)$$

Thus, as  $H_{ca}$  increases from zero,  $\theta_{m2}(H_i)$  increases (or decreases) at first in proportion to  $H_{ca}$ , but finally attains to saturation. This has been recognized experimentally only as an increase of  $\theta_{m2}(H_i)$  with increasing  $H_{ca}$ , which is a part of the experimental fact VII cited before.

### B, Characteristics of the $\theta_a(H_{ca})$ curve.

As may be seen from of Eq. (13), the above considerations made for the characteristics of the  $\theta_a(H_i)$  curve are also valid for those of the  $\theta_a(H_{ca})$  curve, if  $H_i$  and  $H_{ca}$  are interchanged. Thus, we have, in the first place,

$$d\theta_a(H_{ca})/dH_{ca} = (3/a) (H_i/H_a^3) \{ d|\lambda_i(H_a)|/dH_a \} H_{ca}^2 + \{ |\lambda_i(H_a)|/H_a \} (H_i^2 - H_{ca}^2), \quad (23b)$$

and, from this equation,

$$d|\theta_a(H_{ca})|/dH_{ca}|_{H_{ca}=0} = (3/a) \cdot |\lambda_i(H_i)|/H_i, \quad (24b)$$

which indicates that, as  $H_i$  increases from zero, the slope at the origin of the  $\theta_a(H_{ca})$  curve increases (or decreases) from zero, attains a positive maximum (or negative minimum) at  $H_i = H_m^{\lambda/H}$  or  $H_m^{\lambda/H}$  and then decreases (or increases), and, in the IIA (or IIB)-type Wiedemann effect, it afterwards passes through zero at  $H_i = H_0^\lambda$ , attains a negative minimum (or positive maximum) at  $H_i = H_m^{\lambda/H}$ , and finally approaches to zero as  $H_i \rightarrow \infty$ . Experimentally, this has been known only qualitatively and is a part of the above-mentioned experimental fact IX.

Next, the  $\theta_a(H_{ca})$  curve reaches to an extreme value  $\theta_m(H_{ca})$  at  $H_{ca} = (H_{ca})_m^0$  which satisfies the following relation:

$$d|\lambda_i(H_a)|/H_a|_{H_{ca}=(H_{ca})_m^0} = |\lambda_i(H_a)|/H_a|_{H_{ca}=(H_{ca})_m^0} \cdot [ \{ (H_{ca})_m^0 \}^2 - H_i^2 ] / \{ (H_{ca})_m^0 \}^2. \quad (25b)$$

The IA (or IB)-type Wiedemann effect has only one value of  $(H_{ca})_m^0$ ,  $\theta_m(H_{ca})$  being a positive maximum (or negative minimum), while the IIA (or IIB)-type effect has two values of  $(H_{ca})_m^0$ ,  $\theta_{m1}(H_{ca})$  at  $H_{ca} = (H_{ca})_{m1}^0$  and  $\theta_{m2}(H_{ca})$  at  $H_{ca} = (H_{ca})_{m2}^0$  being, respectively, a positive maximum (or negative minimum) and a negative minimum (or positive maximum). Experimentally, the occurrence of  $\theta_m(H_{ca})$  in the IA (or IB)-type Wiedemann effect has not yet been observed because of the above-mentioned smallness of the experimental range of  $H_{ca}$ , but it has been confirmed surely that the rate of increase (or decrease) of  $\theta_a(H_{ca})$  decreases (or increases) with increasing  $H_{ca}$  for small  $H_i$ , which is the remaining part of the above-cited experimental fact IX. While, for iron (or the IIA-type Wiedemann effect), only the occurrence of  $\theta_{m1}(H_{ca})$  for small  $H_i$  has been observed (cf. Fig. 2).

In the whole field range of the IA (or IB)-type Wiedemann effect and in the field range  $0 \leq H_a \leq H_m^\lambda$  of the IIA (or IIB)-type effect, we get, from Eq. (25b),

$$(H_{ca})_m^\lambda \text{ or } (H_{ca})_{m1}^0 \geq H_i \quad \text{for } 0 \leq H_a \leq H_s \text{ or } H_m^\lambda, \quad (26b)$$



and, as  $H_i$  increases from zero,  $(H_{ca})_m^0$  increases from  $H_m^{\lambda/H}$  and, after attaining  $H_s/\sqrt{2}$ , increases in proportion to  $H_i$ , while  $(H_{ca})_{m1}^0$  increases from  $H_m^{\lambda/H}$  and reaches to  $H_m^{\lambda}/\sqrt{2}$ , or

$$H_m^{\lambda/H} < (H_{ca})_m^0 \leq H_s/\sqrt{2} < H_s \quad \text{and} \quad H_m^{\lambda/H} < (H_{ca})_{m1}^0 \leq H_m^{\lambda}/\sqrt{2} < H_m^{\lambda}. \quad (27b)$$

Experimentally, however, only the rise of  $(H_{ca})_{m1}^0$  with increasing  $H_i$  in iron has been known because of the above-mentioned lack of the experimental range of  $H_{ca}$ .

Further, we have, in place of Eq. (28a),

$$\left. \begin{aligned} |\theta_m(H_{ca})| &= (3/a) \{ |\lambda_l(H_a)| / H_a \}_m \cdot H_i & \text{for } H_i \ll (H_{ca})_m^0 \\ \text{and } |\theta_{m1}(H_{ca})| &= (3/a) \{ |\lambda_l(H_a)| / H_a \}_{m1} \cdot H_i & \text{for } H_i \ll (H_{ca})_{m1}^0, \end{aligned} \right\} \quad (28b)$$

and, in place of Eq. (29a),

$$\left. \begin{aligned} |\theta_m(H_{ca})| &= (3/2a) \cdot |\lambda_s| & \text{for } H_i = (H_{ca})_m^0 \geq H_s/\sqrt{2} \\ \text{and } |\theta_{m1}(H_{ca})| &= (3/2a) \cdot |\lambda_m| & \text{for } H_i = (H_{ca})_{m1}^0 = H_m^{\lambda}/\sqrt{2}. \end{aligned} \right\} \quad (29b)$$

Thus, as  $H_i$  increases from zero,  $\theta_m(H_{ca})$  or  $\theta_{m1}(H_{ca})$  increases (or decreases) at first in proportion to  $H_i$ , but then the rate of increase (or decrease) decreases gradually,  $\theta_m(H_{ca})$  or  $\theta_{m1}(H_{ca})$  finally attaining saturation. Experimentally, only it has been found that in iron  $\theta_{m1}(H_{ca})$  increases with increasing but small  $H_i$ .

For the IIA (or IIB)-type Wiedemann effect, we have

$$(H_{ca})_{m1}^0 \leq H_i \quad \text{for} \quad H_m^{\lambda} \leq H_a \leq H_0^{\lambda} \quad (30b)$$

and, as  $H_i$  increases from  $H_m^{\lambda}/\sqrt{2}$ ,  $(H_{ca})_{m1}^0$  decreases from  $H_m^{\lambda}/\sqrt{2}$  and vanishes when  $H_i$  reaches to  $H_0^{\lambda}$ . Also we have

$$|\theta_{m1}(H_{ca})| = (3/a) \cdot |\lambda_l(H_i)| \cdot (H_{ca})_{m1}^0 / H_i \quad \text{for } H_i \gg (H_{ca})_{m1}^0, \quad (31b)$$

indicating that, as  $H_i$  increases from  $H_m^{\lambda}/\sqrt{2}$ ,  $\theta_{m1}(H_{ca})$  decreases (or increases) from  $(3/2a)\lambda_m$  and vanishes at  $H_i = H_0^{\lambda}$ . These are recognized qualitatively with the experimental  $\theta_a(H_{ca})$  curves of iron.

Further more, for the IIA (or IIB)-type Wiedemann effect, we have

$$(H_{ca})_0^0 < H_0^{\lambda} = (H_a)_0^{\lambda} |_{H_i=0} = (H_{ca})_0^{\lambda}. \quad (32b)$$

Thus,  $(H_{ca})_0^0$  or the value of  $H_{ca}$  where  $\theta_a(H_{ca})$  once becomes zero, is always lower than  $(H_{ca})_0^{\lambda}$  or the value of  $H_{ca}$  where the magnetostriction passes through zero, but this has not yet been found experimentally because of the above-mentioned lack of the measured range of  $H_{ca}$ .

Finally, we have

$$(H_{ca})_{m2}^0 \geq H_i \quad \text{for } H_a \geq H_0^{\lambda}, \quad (33b)$$

which indicates that, as  $H_i$  increases from zero,  $(H_{ca})_{m2}^0$  increases from  $H_m^{\lambda/H}$  to  $H_s/\sqrt{2}$  and then increases in proportion to  $H_i$ . We also have

$$|\theta_{m_2}(H_{ca})| = (3/a) \{ |\lambda_i(H_a)| / H_a \}_{m_2} \cdot H_i \quad \text{for } H_i \ll (H_{ca})_{m_2}^0 \quad (34b)$$

$$\text{and } |\theta_{m_2}(H_{ca})| = (3/2a) \cdot \lambda_s \quad \text{for } H_i = (H_{ca})_{m_2}^0 \geq H_s / \sqrt{2}, \quad (35b)$$

which show that, as  $H_{ca}$  increases from zero,  $\theta_{m_2}(H_{ca})$  increases (or decreases) at first in proportion to  $H_i$ , but finally attains to saturation. But, these have not yet been known experimentally on account of the above-mentioned reason concerning  $H_{ca}$ .

#### IV. Quantitative comparison of the theoretical formulae with the experimental data

As described above, Eq. (12) or (13) can explain qualitatively completely all of the experimental facts now available concerning the Wiedemann effect. Then, how is the quantitative comparison? But, it must be noticed that the quantitative comparison between Eq. (12) or (13) and the experimental data can not perfectly be made at present. The reasons are as follows: In the first place, all of  $H_{ca}$ ,  $H_i$  and  $H_a$  in Eq. (12) or (13) are really the effective magnetic fields.  $H_{ca}$  as it is may surely be the effective field and independent of  $z$  (cf. Fig. 6), since the corresponding lines of magnetic force are endless in the interior of the specimen. On the contrary, an externally applied longitudinal field,  $H_{l,ex}$ , may not be the effective field as it stands, since the corresponding lines of force do not close in the interior of the specimen, and hence it is also the case for the field  $H_{a,ex}$  resultant from  $H_{l,ex}$  and  $H_{ca}$ . If the demagnetizing factors in the directions of the lines of forces corresponding to  $H_{l,ex}$  and  $H_{a,ex}$  are denoted, respectively, as  $N_l$  and  $N_a$ , we have the following formal relations:

$$H_i(z) = H_{l,ex} - N_l(I_l)I_l(z) \quad (36a)$$

and

$$H_a(z) = H_{a,ex} - N_a(I_a)I_a(z). \quad (36b)$$

Consequently,  $\theta_a$  as given by Eq. (12) or (13) is a function of  $z$ , and Eq. (12) or (13) at once gives  $\theta_a$  for the entire of the specimen only when  $H_i$  is uniform over the entire specimen, namely, when the length of the specimen is infinite.

But, since the actual measurements of the Wiedemann effect are made with the entire of the circular rod or tube specimen of the finite length, the measured value,  $\theta_{meas}$ , is the value of  $\theta_a$  averaged over the entire length  $L$  of the specimen,  $\bar{\theta}_a$ , or

$$\theta_{meas} = \bar{\theta}_a = 3(H_{ca}/a) \cdot \overline{\{ \lambda_i(H_a) \cdot (H_i/H_a^2) \}}, \quad (37)$$

where

$$\bar{x} = (1/L) \int_0^L x dz. \quad (38)$$

Since it is at present difficult or even impossible to give simple analytical expressions for  $H_i(z)$ ,  $H_a(z)$ , and  $\lambda_i(z)$ , it is impossible to give theoretically the value of  $\overline{\lambda_i(H_a) \cdot (H_i/H_a^2)}$ , which is not given experimentally, too. Thus, the quantitatively perfect comparison between theory and experiment on the Wiedemann

effect can not be made.

Now, in order to make a quantitative, though incomplete, comparison, we put

$$\overline{\lambda_i(H_a)} \cdot (\overline{H_i}/H_a^2) = \overline{\lambda_i(H_a)} \cdot \overline{H_i} / \{(\overline{H_i})^2 + H_{ca}^2\}, \quad (39)$$

and

$$\overline{\lambda_i(H_a)} = \overline{\lambda_i(\overline{H_i})} \Big|_{\overline{H_i}=H_a} \quad (40)$$

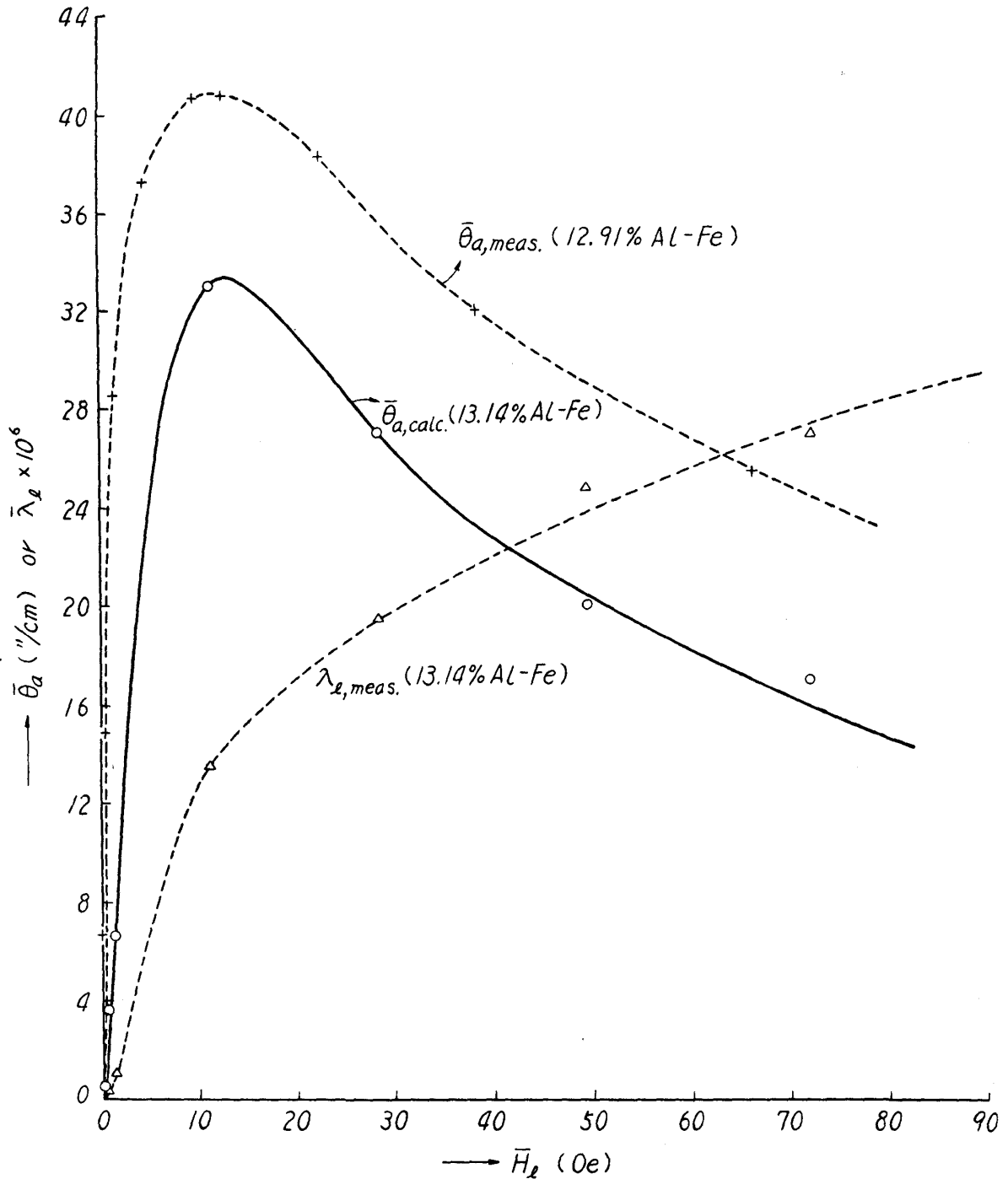


Fig. 9. Theoretical  $(\overline{\theta}_a - \overline{H}_i)$  curve for  $H_{ca} = 10.7$  Oe of 13.14 %Al-Fe alloy as compared with the measured curve of 12.91 %Al-Fe alloy<sup>(9)</sup> (both cylindrical rod specimens). The measured  $(\overline{\lambda}_l - \overline{H}_i)$  curve of the former alloy<sup>(12)</sup> as employed for the calculation of the  $(\overline{\theta}_a - \overline{H}_i)$  curve is also shown.

or that  $\overline{\lambda}_l(H_a)$  is equal to the longitudinal magnetostriction measured over the entire length of specimen in which the mean effective magnetic field equal to  $H_a$  is applied along the rod axis. Then, Eq. (37) is reduced to

$$\theta_{meas} = \overline{\theta}_a = (3/a) \cdot \overline{\lambda}_l(\overline{H}_l) \Big|_{\overline{H}_l = H_a} \cdot H_{ca} \overline{H}_l / \{ (\overline{H}_l)^2 + (H_{ca})^2 \}. \quad (41)$$

$\theta_a$  referred to above is expressed in the unit of radians/cm, but experimentally it is usually expressed in the unit of  $\mu$ /cm. So, using the factor  $4.85 \times 10^{-6}$  to convert radian to  $\mu$ , Eq. (41) is written as

$$\theta_{meas} (\mu/cm) = \overline{\theta}_a (\mu/cm) = (0.619 \times 10^{-6}/a) \cdot \overline{\lambda}_l(\overline{H}_l) \Big|_{\overline{H}_l = H_a} \cdot H_{ca} \overline{H}_l / \{ H_{ca}^2 + (\overline{H}_l)^2 \}. \quad (41a)$$

We have made such a concession theoretically, but there is yet a difficulty on the experimental side. The experiments that can be compared with Eq. (41a) should be those which measured the Wiedemann effect and longitudinal magnetostriction with the same specimens and, moreover, provide the data of  $\overline{\theta}(\overline{H}_l)$  and  $\overline{\lambda}_l(\overline{H}_l)$ , but such experiments are not available. Then, we conceded to a larger extent, and searched for experiments which measured  $\overline{\theta}(\overline{H}_l)$  and  $\overline{\lambda}_l(\overline{H}_l)$  with similar substances.

Such experiments are Honda, Masumoto, Shirakawa, and Kobayashi's<sup>(16)</sup> measure-

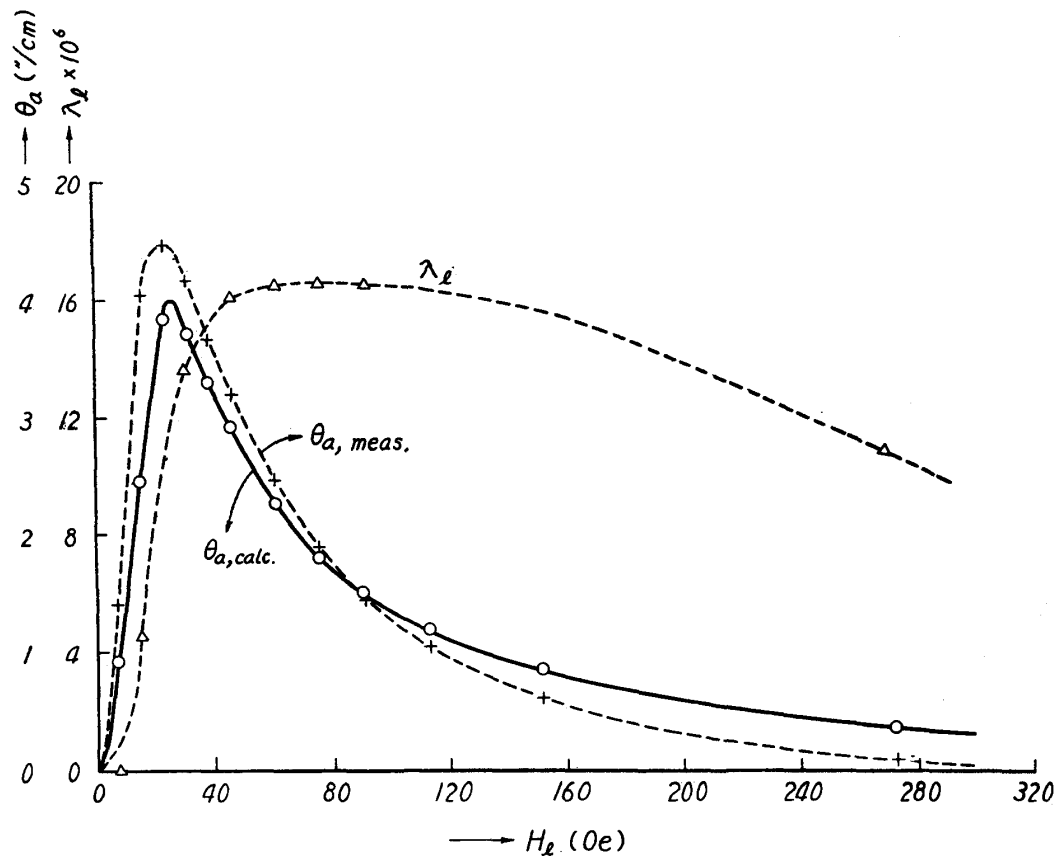


Fig. 10. Theoretical  $(\theta_a - H_l)$  curve for  $H_{ca}$  2.04 Oe of a cylindrical tube specimen of low-carbon steel as compared with the measured curve.<sup>(4)</sup> The measured  $(\lambda_l - H_l)$  curve<sup>(4)</sup> as used for the calculation of the  $(\theta_a - H_l)$  curve is also shown.

(16) K. Honda, H. Masumoto, Y. Shirakawa and T. Kobayashi, Nippon Kinzoku Gakkai-shi, 12 (1948), No. 7-12; Sci. Rep. RITU, A1 (1949), 341.

ments of  $\overline{\lambda}_l(\overline{H}_l)$  with an iron-aluminum alloy containing 13.14 %Al ( $a = 0.2$  cm,  $L = 10$  cm; annealed at  $1000^\circ\text{C}$  for 1 hour in vacuo) and Shirakawa, Ohara and Abe's<sup>(9)</sup> measurements of  $\overline{\theta}(\overline{H}_l)$  with an iron-aluminum alloy containing 12.91 %Al ( $a = 0.15$  cm,  $L = 15$  cm; annealed at  $1000^\circ\text{C}$  for 1 hour) alone. It may be seen from Fig. 9 that the values of  $\overline{\theta}_a(\overline{H}_l)$  for, for example,  $a = 0.15$  cm and  $H_{ca} = 10.7$  Oe calculated using Eq. (41a) from the measured data for  $\overline{\lambda}_l(\overline{H}_l)$  of the former experiments (cf. Fig. 9) are in a quantitatively good agreement with the measured data for  $\overline{\theta}_a(\overline{H}_l)$  of the latter experiments.

Further, we have William's<sup>(4)</sup> experiments which measured  $\lambda_l(H_{l,ex})$  and  $\theta_a(H_{l,ex})$  with a very slender cylindrical-tube specimen of low-carbon steel (outer radius 0.2386 cm, inner radius 0.1538 cm,  $L = 80.2$  cm; heat-treatment unknown). In this case, we may regard  $H_{l,ex} = H_l$  and  $H_{a,ex} = H_{ca}$ , so that  $\lambda_l(H_{l,ex}) = \lambda_l(H_l)$ ,  $\lambda_l(H) = \lambda_l(H_l)|_{H_l=H_a}$ , and  $\theta_a(H_{l,ex}) = \theta_a(H_l)$ , and hence Eq. (41a) becomes

$$\theta_{meas}(\text{ } / \text{cm}) = \theta_a(\text{ } / \text{cm}) = (0.619 \times 10^{-6}/a) \cdot \lambda_l(H_l)|_{H_l=H_a} \cdot H_l H_{ca} / (H_l^2 + H_{ca}^2). \quad (41b)$$

The values of  $\theta_a$  for  $H_{ca} = 2.04$  Oe, calculated using Eq. (41b) from the measured data of  $\lambda_l(H_l)$  (Fig. 10), taking  $a = (1/2)$ (outer radius + inner radius), are compared with the measured data for  $\theta_a$  in Fig. 10, which shows that the computed and measured data agree well with each other.

### Summary

As regards the classical problem of the Wiedemann effect in ferromagnetic polycrystalline substance, any satisfactory theory has not yet been proposed, except Fromy's<sup>(8)</sup> theory for the case of a thin-walled circular tube specimen which has been almost entirely neglected in the literature. The author has developed a general theory of the effect for the case of a cylindrical rod specimen, which involves Fromy's theory as a limiting case.

When a ferromagnetic cylindrical-rod specimen with the diameter  $a$ , which is fixed at its one end, is magnetized under longitudinal magnetic field,  $H_l$ , parallel to, and circular field,  $H_c$ , around, the rod axis, the resultant magnetic field,  $H_r$ , at a point P in the specimen apart from the rod axis by the distance  $r$ , is given by  $(H_l^2 + H_{cr}^2)^{1/2}$ , ( $H_{cr}$  is the value of  $H_c$  at P), pointing to a direction which makes an angle  $\varphi_r = \tan^{-1}(H_{cr}/H_r)$  against the direction of  $H_l$ . The magnetization,  $I_r$ , at P takes a direction for which the sum of the magnetic field and elastic energies is minimum and thus the direction of  $I_r$  generally does not coincide with that of  $H_r$  but makes a small angle  $\varepsilon_r$  with the direction of  $H_r$  in the  $(H_l, H_{cr})$  plane. Of the components of the magnetostrictive strain tensor, associated with  $I_r$ , referred to the cylindrical coordinate system  $(r, z, \theta)$ , of which the  $z$  axis is the rod axis and the  $r$  axis is the direction of radius passing through P,  $e_{rr}$ ,  $e_{\theta\theta}$ ,  $e_{22}$ , and

$$e_{\theta z} = 2\{\lambda_t(I_r) - \lambda_l(I_r)\} \cdot I_{rl} I_{rc} / I_r^2 \quad (7)$$

are not zero, where  $\lambda_l(I_r)$  and  $\lambda_t(I_r)$  are, respectively the longitudinal and transverse magnetostrictions associated with  $I_r$ ,  $I_{rl} = I_r \cos(\varphi_r + \varepsilon_r)$ , and  $I_{re} = I_r \sin(\varphi_r + \varepsilon_r)$ .  $e_{\theta z}$  expresses the shear of unit volume at P along the direction of the rod axis and that along the direction normal to it and the unit volume may be regarded as fixed at its one face normal to the direction of the rod axis, so that  $e_{\theta z}$  results the torsion

$$\theta_r = e_{\theta z}/r = (2/r) \{ \lambda_l(I_r) - \lambda_t(I_r) \} \cdot I_{rl} I_{re} / I_r^2, \quad (8)$$

this torsion being the Wiedemann effect.

For normal ferromagnetic substances, in which the elastic energy is far smaller than the magnetic field energy and hence the direction of  $I_r$  practically coincides with that of  $H_r$ , Eq. (8) may be written as

$$\theta_r = (2/r) \{ \lambda_l(H_r) - \lambda_t(H_r) \} \cdot H_l H_{er} / H_r^2, \quad (11)$$

which becomes, for the surface of the rod,

$$\theta_a = (2/a) \{ \lambda_l(H_a) - \lambda_t(H_a) \} \cdot H_l H_{ca} / H_a^2. \quad (12)$$

Eq. (12), which holds also for a thin-walled circular tube, is the expression derived already by Fromy<sup>(8)</sup> through an elementally and hence lengthy consideration.

Eq. (12) or (13) indicates that the Wiedemann effect in circular rod or tube specimens is determined uniquely by the radius of the specimen and its magnetostriction characteristics. The magnetostriction characteristics are generally divided into two types, in one of which the magnetostriction increases (or decreases) monotonously over the entire field range and in the other of which the magnetostriction shows a positive maximum (or negative minimum) at low fields, then passes through zero, and changes its sign, so that the Wiedemann effect may have the corresponding two types. Changing one of  $H_l$  and  $H_c$  at fixing the other, the Wiedemann effect of the first type shows a sharp positive maximum (or negative minimum) at low fields and then approaches to zero at high fields, while the second type, after attaining a sharp positive maximum (or negative minimum), passes through zero, shows a flat negative minimum (or positive maximum), and then vanishes at high fields. The first-type Wiedemann effect is that of nickel and cobalt, and the second-type effect is that of iron and alfer (13 %Al-Fe alloy).

These two types of the Wiedemann effects have been analysed detailedly using simple Eq. (13). Thus it has been shown that all of the available experimental facts concerning the Wiedemann effect of cylindrical rod and tube specimens can be explained qualitatively perfectly and, moreover, it has been predicted that several new facts would be observed if the experiments could be made under high circular field. Finally, the quantitative comparison with experimental facts made under a more or less reasonable assumption has shown a pretty well agreement.

In closing, the author wishes to express his hearty thanks to Mr. T. Iwata and Dr. S. Taniguchi who gave him valuable discussions throughout this work.